

CNMBI: Determining the Number of Clusters Using Center Pairwise Matching and Boundary Filtering

Ruilin Zhang¹, Haiyang Zheng¹, and Hongpeng Wang^{1(†),2}

¹ Harbin Institute of Technology, Shenzhen, Shenzhen, China
wanghp@hit.edu.cn

² Peng Cheng Laboratory, Shenzhen, China

Abstract. One of the main challenges in data mining is choosing the optimal number of clusters without prior information. Notably, existing methods are usually in the philosophy of cluster validation and hence have underlying assumptions on data distribution, which prevents their application to complex data such as large-scale images and high-dimensional data from the real world. In this regard, we propose an approach named CNMBI. Leveraging the distribution information inherent in the data space, we map the target task as a dynamic comparison process between cluster centers regarding positional behavior, without relying on the complete clustering results and designing the complex validity index as before. Bipartite graph theory is then employed to efficiently model this process. Additionally, we find that different samples have different confidence levels and thereby actively remove low-confidence ones, which is, for the first time to our knowledge, considered in cluster number determination. CNMBI is robust and allows for more flexibility in the dimension and shape of the target data (e.g., CIFAR-10 and STL-10). Extensive comparison studies with state-of-the-art competitors on various challenging datasets demonstrate the superiority of our method.

Keywords: Number of clusters · Cluster center · Complex data · Pairwise matching · Boundary filtering.

1 Introduction

The automatic determination of parameters has become one of the main considerations for the popularity of a learning solution in machine learning or pattern recognition[25]. Clustering, as an essential analysis tool, endeavors to discover underlying structure from unlabeled data, ensuring that samples³ in the same group have high homogeneity and that different groups have the maximum difference[29]. It should be noted that, typically, most clustering approaches suffer from the limitation that the number of clusters has to be fed by a human user, which is fundamental to obtaining a good data partition. However, the number

³ Data points, objects, and samples are used interchangeably in this paper.

of clusters in practice is usually unknown, as Salvador stated in [38], which often results in suboptimal clustering results. Determining the number of clusters automatically can enhance the potential of clustering methods, while also being instructive for other learning tasks, like counting the amount of farmland in remote sensing images and setting the type of anchors in object detection[33]. Although several solutions[4,53,1,43] have recently been proposed to estimate the number of clusters, they either perform unstably or are challenging to employ in practice when handling complex data like large-scale images and high-dimensional data from the real world. Technically, existing methods are generally based on the clustering validation philosophy, which uses the quality of clustering results to reveal the number of clusters, i.e., evaluating a clustering validity index (named CVI) over the target data and optimizing it as a function of the number of clusters. With a clear semantic and mathematical background, this paradigm has gained significant attention[37,28], mainly covering the design of cluster validity index (CVI)[49,53,37] and the embedding of clustering schemes[4,43,33].

Nevertheless, the unsupervised context limits existing methods to design CVI based solely on the subjective morphological characteristics of final clusters, such as compactness and separation, which inevitably imposes potential assumptions on the target data distribution. Moreover, the clustering results of each round during iterative optimization are sometimes not discriminative and instructive, as in the case of complex data, due to the inherent limitations of the chosen clustering scheme. Commonly used K-means, for instance, favors spherical or well-separated clusters, so the consistency of the optimal number of clusters, the best clustering result, and the best score, i.e., the philosophy underlying such methods, could be invalidated by some challenging data. Additionally, we observe that existing work generally focuses on the methodological level while ignoring the significance of the sample to the target task in practice.

With this in mind, we bridge these bottlenecks by proposing a novel algorithm (CNMBI). Our work demonstrates the following contributions:

- 1) We propose a scheme for determining the number of clusters based on center pairwise matching. Instead of previous approaches resorting to CVI scoring and complete clustering results, we use inherent distribution information in the data space to model cluster number determination as a dynamic contrastive process of cluster centers regarding positional behavior.
- 2) We develop a boundary filtering method to remove low-confidence samples that interfere with the cluster number determination task, allowing our method to have greater flexibility and robustness in terms of data shape and dimension. To the best of our knowledge, this aspect has not been considered.
- 3) Our method outperforms the state-of-the-art competitors on diverse benchmark datasets (e.g., STL-10, MNIST, and CIFAR-10), and we are the first to report the results of a cluster number determination method on the challenging dataset such as STL-10 and CIFAR-10. The in-depth discussions of boundary information, and robustness jointly demonstrate the superiority of CNMBI.

2 Related Work

For the goal of determining the number of clusters, the philosophy behind most methods is that the actual number of clusters, the best clustering result, and the best clustering validity score are consistent. In this context, designing an effective validity index is essential because the optimal number of clusters needs to be reflected by evaluating the clustering results. Conventionally, most CVIs take distance information of resulting clusters as the main focus, considering the intra-cluster distance (compactness), inter-cluster distance (separation), or the statistical variants of both to describe clustering results, such as DBI[5], DUNN[6], CH[3]. Combined with partition-based clustering, these indexes can suggest the desired number of clusters under the spherical or well-separated data. Additionally, some work attempts to construct various curves formed by intra-cluster variance, using characteristics such as "maximum curvature"[56], "knee of the curve"[38], "elbow of the curve", "max magnitude"[45], or "sharp jump"[42] to visually locate the number of clusters.

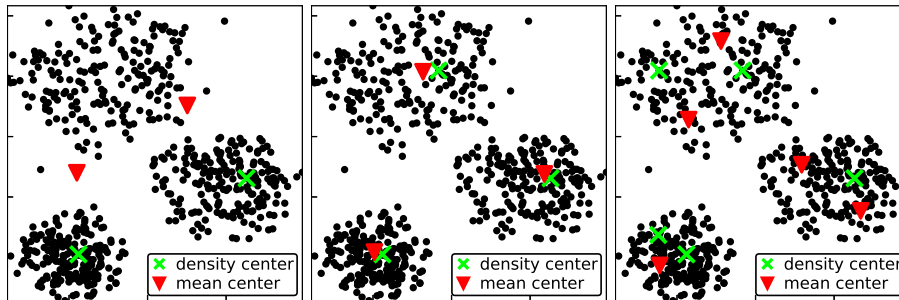
Recently, in addition to the work above relying on distance information, several efforts have leveraged density information to define CVI or update clustering schemes. For instance, [43] uses cluster density to evaluate the clustering results. Likewise, LCCV [4] selects a group of highly representative density cores by density information to simplify the silhouette coefficient and employs agglomerative hierarchical clustering as the assignment scheme. Besides, there are some promising density clustering methods that work with CVI, one of the typical paradigms is density peaks clustering (DPC)[34]. As in the case of [49], which simplifies the adapted silhouette coefficient by considering density centers from DPC as representative. Another example is DPC-AHS[53], which takes the skew of distribution within the cluster as the validity index by the advantages of density clustering for arbitrary-shaped data. Despite their simplicity and ease of implementation, these methods are not practical as they usually perform unstably on some complex data such as large-scale images and high-dimensional data from the real world, as discussed in the introduction. In contrast, our method addresses the above limitations.

3 Proposed Method: CNMBI

3.1 Center-Pairwise Matching

Cluster number determination is essentially a dynamic optimization process, so one potential solution is to improve identification performance by leveraging valuable pattern information. However, in such an unsupervised context, significant external information, such as data labels, is unavailable. It should be noted that the distribution information from the data space is also instructive, such as the cluster center generated by density or geometric information, which is closely related to the number of clusters and, more importantly, is the most representative in the data space.

With this in mind, we find a fundamental insight that the distance between the density centers (using density information) and the mean centers (relying geometric information) is closest when and only when the number of clusters is actual, which is enlightening for cluster number determination. As shown in Fig. 1, the distances between the mean centers and the density centers are small and the positions almost overlap in the case of the number of clusters $k = 3$. On the contrary, there is a significant distance between the two in cases smaller than the actual number of clusters (Fig. 1(a), $k=2$) or larger (Fig. 1(c), $k=5$). To further discuss the principle behind this observation above, we have some formal definitions as follows.



(a) case 1: $k = 2 < K = 3$. (b) case 2: $k = K = 3$. (c) case 3: $k = 5 > K = 3$.

Fig. 1: Density center versus mean center for different cluster number settings.

Given a dataset $X \in \mathbb{R}^d$ containing K actual clusters of n samples. Let k denote the number of clusters currently under consideration, the mean center is obtained by

$$S_{\mu}^{(k)} = \left\{ \frac{\sum_{x \in C_{\mu}^{(i)}} x}{|C_{\mu}^{(i)}|} \mid 1 \leq i \leq k \right\} \quad (1)$$

where $S_{\mu}^{(k)}$ represents a set containing k mean centers and $C_{\mu}^{(i)}$ denotes a cluster generated by partitioning-based clustering (K-means is used here), i.e. $X = \{C_{\mu}^{(1)}, \dots, C_{\mu}^{(k)}\}$. In particular, Eq. (1) illustrates that the mean centers are geometric centroids of the resulting clusters and their positions are unstable. As shown in Fig. 1, in the case of $k=2$ or $k=5$, the mean centers are generally distributed at the edges or outside of the actual clusters in X , due to cluster splitting or cluster merging behaviors.

In addition, the density centers are described as those objects surrounded by neighbors with lower density and have a relatively large distance from any data points with higher density, as discussed in DPC. To this aim, the two quantities: local density ρ and δ distance are used to measure the possibility of each object

becoming a cluster center from the density view.

$$\rho_i = \sum_{x_j \in X \setminus \{x_i\}} \exp\left(-\left(\frac{d_{ij}}{dc}\right)^2\right) \quad (2)$$

$$\delta_i = \begin{cases} \min\{\text{dist}(x_i, x_j) \mid \rho_i < \rho_j, x_i \in X\} & \text{if } \exists x_j \in X, \rho_i < \rho_j \\ \max\{\text{dist}(x_i, x_j) \mid x_j \in X\} & \text{otherwise} \end{cases} \quad (3)$$

Where dc acts as the sampling radius of density calculation, it is determined by sorting n^2 distances in X from ascending order and selecting a number ranked at 2%. With the product $\gamma_i = \rho_i \times \delta_i$, the greater the score γ_i , the more likely the x_i is considered as a cluster center.

Definition 1. Density Center Set Given the current cluster number k , the density center set $S_\gamma^{(k)}$, including k centers determined by DPC, is given by

$$S_\gamma^{(k)} = \{y_i \mid \gamma_i \geq \bar{\gamma}_k, 1 \leq i \leq n\} \quad (4)$$

where $\bar{\gamma}_k$ is the k -th largest gamma score by sorting objects in γ descending order. Note that the cardinality of both sets $S_\gamma^{(k)}$ and $S_\mu^{(k)}$ is k . According to the above formula, we can also conclude that the density center tends to be the most core region of each actual cluster in X , and the position is stable because the density information directly determines it.

Inspired by above observation, we draw a promising insight favoring the determination of the number of clusters: "the difference between the mean center and the density center in terms of location distribution is minimal when and only when the actual number of clusters is given, quantified as the sum of the k pairwise distances formed is minimal compared to the other cases".

To apply this insight, we propose to model the relationship between the density centers and mean centers using graph theory to quantify the actual distance between them. The solution regarding the optimal number of clusters can be transformed into the searching the "Center Pairwise Matching" below.

We formally treat Mean Center Set S_μ (following Eq. (1)) and Density Center Set S_γ (following Eq. (4)) as two graph node sets, and the elements of which are regarded as individual nodes. After that, Center Bipartite Graph is defined as.

Definition 2. Center Bipartite Graph Let $S_\gamma^{(k)}$ and $S_\mu^{(k)}$ be the set of mean center and density center at number of clusters k , respectively. We then define the center bipartite graph $G_{\mu,\gamma}^{(k)} = (V^{(k)}, E^{(k)})$ such that it should obey the properties:

(1) $V^{(k)} = \{S_\mu^{(k)} \cup S_\gamma^{(k)}\}$ and $S_\mu^{(k)} \cap S_\gamma^{(k)} = \emptyset$; (2) for each node $x_i \in S_\mu^{(k)}$ (or $x_j \in S_\gamma^{(k)}$), there must be k edges between it and another node subset; (3) for each edge $e(x_i, x_j) \in E^{(k)}$, that means $x_j \in S_\mu^{(k)}$ as well as $x_j \in S_\gamma^{(k)}$.

Definition 3. Center Complete Matching Let CM represent a complete matching on $G_{\mu,\gamma}^{(k)} = (V^{(k)}, E^{(k)})$, a subset of size k of the edge set E^k , which must satisfy the following conditions:

(1) For any two edges $e(x_i, x_j), e(x_p, x_q) \in CM$, $x_i \cap x_p = \emptyset$ and $x_j \cap x_q = \emptyset$ should be hold; (2) $|CM| = |S_\gamma^{(k)}| = |S_\mu^{(k)}|$. Note that for the graph $G_{\mu, \gamma}^{(k)}$, there are $k!$ complete matching cases: $CM \in P^{(k)} = \{M_1, M_2, \dots, M_{k!}\}$.

Definition 4. Center Similarity Matrix For any complete matching $PM \in P^{(k)}$ of the center bipartite graph $G_{\mu, \gamma}^{(k)}$, the corresponding "center similarity matrix" with sparse property, denoted by CD , is defined as:

$$CD_{[p,q]}^{(k)} = \begin{cases} \|x_p - x_q\|_2^2, & \text{if } e(x_p, x_q) \in CM \\ 0 & \text{otherwise} \end{cases} \quad (5)$$

Definition 5. Center Pairwise Loss Given a matching scheme CM , the expectation of center similarity matrix CD , called "center pairwise loss", is used to quantify the center pairwise relationships in this matching CM

$$L(CM) = \frac{1}{k} I_{1*k} (CD^{(k)}) * I_{1*k}^T \quad (6)$$

where $I_{1*k} = (1, 1, \dots, 1)_{1*k}^T$ is an auxiliary matrix for vectorization.

Definition 6. Center Pairwise Matching Given the number of clusters k , there exist K_i complete matches between the mean center and the density center. We use the "center pairwise matching" as the matching scheme under the current number of clusters, expressed as follows.

$$CPM^{(k)} = \left\{ \bigcup_{e(x_p, x_q) \in PM} e(x_p, x_q) \mid \arg \min_{PM \in P^{(k)}} (L(PM)) \right\} \quad (7)$$

It is worth mentioning that the loss value of the center pairwise matching is considered as the unique feature value of the current number of clusters during cluster number optimization. To this end, the optimal number of clusters should be projected as the global minimum center loss, thus we define

$$K^* = \arg \min_k (L(CPM^{(k)})) \quad (8)$$

3.2 Low Confidence Sample Filtering

Inspired by self-paced learning in which samples have different confidence levels for a given learning task, we note that some extreme points in the data space, especially at the edges of clusters, between clusters, or away from clusters, may disturb the cluster number identification. These points do not reveal the core structure of the clusters as well as tend to incur cluster merging, weaken the independence of clusters, eventually breaking the consistency between "the actual number of clusters," "the best clustering result," and "the best score," which is the main factor that current work is hard to deal with complex data. It is noteworthy that the existing methods are not aware of this fact. To this aim,

we propose a boundary filtering method based on space vector decomposition, aiming to enhance the robustness of our method against complex data.

We find that the boundary object and its neighbors have strong unbalance in the projection subspace, forming the typical skew distribution in the direction of the base vector. By contrast, the neighbors of the core object show significant symmetry in the direction of the basis vector[54]. With this in mind, we first treat the close relationship between target object and its neighbors as independent space vectors, described as follows.

Let x_i be any object in data set $X = \{x_1, x_2, \dots, x_n\} \in \mathbb{R}^{m \times n}$. According to the space vector decomposition theorem, there exists a unique ordered sequence of real number $\{\lambda_1, \lambda_2, \dots, \lambda_m\}$ such that $x_i = \lambda_1 e_1 + \lambda_2 e_2 + \dots + \lambda_m e_m$, where $\{e_1, e_2, \dots, e_m\}$ denotes the basis vectors for the data space \mathbb{R}^m . For $\forall x_i, x_j \in X$, the neighborhood vector formed by the two in \mathbb{R}^m is given by

$$h_{i,j} = (\lambda_{i,1} - \lambda_{j,1}, \dots, \lambda_{i,d} - \lambda_{j,d}, \dots, \lambda_{i,m} - \lambda_{j,m})(e_1, \dots, e_m)^T \quad 1 \leq i, j \leq n \quad (9)$$

where $\lambda_{i,d} - \lambda_{j,d}$ denotes the projection of $h_{i,j}$ in the direction of basis vector e_d .

Notably, the neighbors of x_i refers to objects within the open neighborhood of x_i with the radius as dc , i.e., $N_{dc}(x_i)$. As the typical operation to describe spatial position relations, the local representative vector \mathcal{H}_i is customized as the vector addition regarding x_i and its neighbors.

$$\mathcal{H}_i = \sum_{x_j \in N_{dc}(x_i)} (h_{i,j}) = \left(\sum_{x_j} (\lambda_{i,1} - \lambda_{j,1}), \dots, \sum_{x_j} (\lambda_{i,m} - \lambda_{j,m}) \right) (e_1, \dots, e_m)^T \quad (10)$$

where $\sum (\lambda_{i,d} - \lambda_{j,d})$ symbolizes the projection of the neighborhood vectors of x_i in the direction of the basis vector e_d . In this regard, we make the following derivation about projection of the neighborhood vector onto the feature space:

Theorem 1. *Given a one-dimensional feature space $v_d (1 \leq d \leq m)$ and the neighborhood vector $h_{i,j}$, then the projection of the neighborhood vector $h_{i,j}$ onto it is $e_d(e_d^T e_d)^{-1} e_d^T h_{i,j}$, where e_d is the basis vector of v_d .*

Proof. Assuming \mathcal{S} is a subspace of \mathbb{R}^m ($\mathcal{S} \in \mathbb{R}^p$, s.t. $p \leq m$) and $\{e'_1, e'_2, e'_3, e'_4, \dots, e'_p\}$ is a basis, then for any object $a \in \mathcal{S}$, there is only $a = y_1 e'_1 + y_2 e'_2 + y_3 e'_3 + y_4 e'_4 + \dots + y_p e'_p$. Let matrix $A = [e'_1, e'_2, e'_3, e'_4, \dots, e'_p]_{m \times p}$, then $a = Ay$, $y \in \mathbb{R}^p$.

According to the above statement, let $Proj_{\mathcal{S}} h_{i,j}$ denote the projection of neighborhood vector $h_{i,j}$ (composed of $x_i \in \mathbb{R}^m$ and its neighbor $x_j \in \mathbb{R}^m$) on subspace \mathcal{S} , then $Proj_{\mathcal{S}} h_{i,j} \in \mathcal{S}$ with

$$Proj_{\mathcal{S}} h_{i,j} = Ay, y \in \mathbb{R}^p \quad (11)$$

Based on the fundamental theory of linear algebra, the neighborhood vector $h_{i,j}$ is such that $h_{i,j} = Proj_{\mathcal{S}^\perp} h_{i,j} + Proj_{\mathcal{S}} h_{i,j}$, where $Proj_{\mathcal{S}^\perp} h_{i,j}$ denote the projection of $h_{i,j}$ on the orthogonal complement of subspace \mathcal{S} , which is equal to the null space of A^T . We have:

$$Proj_{\mathcal{S}^\perp} h_{i,j} = h_{i,j} - Proj_{\mathcal{S}} h_{i,j} \in Null(A^T) \quad (12)$$

Left-multiplying both sides by A^T and simplifying, we obtain $A^T h_{i,j} - A^T A y = 0$, then $y = (A^T A)^{-1} A^T h_{i,j}$. Substituting the expression for y in the $Proj_s h_{i,j}$, we have $Proj_s h_{i,j} = Ay = A(A^T A)^{-1} A^T h_{i,j}$. Now, Eq. (11) can be rewritten as

$$Proj_s h_{i,j} = Ay = A(A^T A)^{-1} A^T (x_i - x_j) \quad (13)$$

Without loss of generality, we assume that the subspace \mathcal{S} is instantiated as a one-dimensional space s_d , thus the matrix A could be transformed into a column vector e_d , i.e. the basis vector of this one-dimensional space. Consequently, projection is formalized as $e_d(e_d^T e_d)^{-1} e_d^T h_{i,j}$. The theorem is proved. \square

With the help of orthogonality, we utilize a standard orthogonal basis $\{e_d\}_{1 \leq d \leq m}$, (s.t. $\langle e_i, e_j \rangle = 0 \cap e_i^T e_i = 1$), to instantiate matrix A in Eq. (13). After that, the projections of the neighborhood vector $h_{i,j}$ composed of x_i and x_j on the directions of the m orthogonal basis vectors can be expressed as:

$$Proj_{v_d} h_{i,j} = (e_d(e_d^T e_d)^{-1} e_d^T h_{i,j}) = (e_d e_d^T x_i - e_d e_d^T x_j) = (x_{id} - x_{jd}), 1 \leq d \leq m \quad (14)$$

Thus, local representative vector from Eq. (10) is formalized as follows:

$$\begin{aligned} \mathcal{H}_i &= \left(\sum_j Proj_{v_1} h_{i,j}, \sum_j Proj_{v_2} h_{i,j}, \dots, \sum_j Proj_{v_m} h_{i,j} \right) (e_1, e_2, e_3, \dots, e_m)^T \\ &= \left(\sum_j e_1 e_1^T x_i - e_1 e_1^T x_j, \sum_j e_2 e_2^T x_i - e_2 e_2^T x_j, \dots, \sum_j e_m e_m^T x_i - e_m e_m^T x_j \right) \begin{bmatrix} 1 & 0 & \dots & 0 \\ 0 & 1 & 0 & \dots \\ \dots & 0 & 1 & 0 \\ 0 & \dots & 0 & 1 \end{bmatrix} \\ &= \left(\sum_j x_{i1} - x_{j1}, \sum_j x_{i2} - x_{j2}, \dots, \sum_j x_{im} - x_{jm} \right) \end{aligned} \quad (15)$$

Mathematically, the length of the local representative vector \mathcal{H} formed by the boundary object is significantly longer than that of the core object. In this case, the P-norm is preferred here.

Definition 7. Boundary degree Considering the computational cost, the Boundary degree φ is defined by Eq. (16) with $p=1$.

$$\varphi_i = \|\mathcal{H}_i\|_p = \left(\sum_d \left(\left| \sum_j x_{id} - x_{jd} \right| \right)^p \right)^{\frac{1}{p}} \quad \text{s.t. } 1 \leq d \leq m, x_j \in N_{dc}(x_i) \quad (16)$$

where the role of boundary degree φ is to determine whether x_i is a boundary point; a larger value suggests that x_i should be removed first.

After that, the dataset X can be evolved into a core subset:

$$X' = \{x_i \in X : \varphi_i \leq A_\varphi[[n * \lambda]]\} \quad (17)$$

where λ denotes the proportion of low confidence sample in X and A is a descending list of φ . λ is empirically set to 10%. Subsequently, the density centers and mean centers are derived from X' by CNMBI, which finally predicts the number of clusters by the proposed center pairwise matching. As summarized in Algorithm 1.

Algorithm 1: CNMBI

Input: Input data: X
Output: the optimal number K^*

- 1 Calculate Boundary degree of each sample in X , φ_i using Eq. (16) ;
- 2 Remove the low-confidence samples to form the core set X' of X using Eq. (17);
- 3 **for** $k = \hat{k}_{\min} : \hat{k}_{\max}$ **do**
- 4 Find the density center set $S_\gamma^{(k)}$ using Eq. (4)
- 5 Find the mean center set $S_\mu^{(k)}$ using Eq. (1)
- 6 Construct the Center Bipartite Graph $G_{\mu,\gamma}^{(k)}$ using Definition 2
- 7 Search the Center Complete Matching CM and calculate the Center Pairwise Loss $L(CM)$ using Definition 3 and Eq. (7)
- 8 Determine the Pairwise Matching $CPM^{(k)}$ under the k using Eq. (7)
- 9 **end**
- 10 $K^* = \arg \min(L(CPM^{(k)})), k \in [\hat{k}_{\min}, \hat{k}_{\max}]$

Result: K^*

4 Experiments

Data Sets. To demonstrate the effectiveness of the proposed CNMBI, a variety of data scenarios are covered, the information of which is presented in Table 1. The 8 synthetic datasets are generated from Shape sets of the Clustering basic benchmark⁴, and 3 high-dimensional datasets are obtained from the UCI [2]. The image datasets (CIFAR-10⁵, STL-10⁶, MNIST⁷, Pendigits, Optical Recognition, and Pointing⁸) are considered. **Evaluation Metrics.** We record the optimal number of clusters (NC) and calculate the accuracy metric (ACC: i.e., the proportion of successful estimates in 50 runs). **Experimental Settings.** We set the number of clusters k to the acknowledged range of 2 to \sqrt{n} , performing 50 runs. We compare the proposed CNMBI with 4 state-of-the-art approaches, LCCV[4], VCIM[1], DPC-AHS[53], CNAK[37] and well-known validity index SC[35].

4.1 Quantitative Study

Table 2 summarizes the experimental results of the quantitative study, from which we can draw some conclusions. First, our algorithm correctly identified 13 out of 17 datasets in 50 runs, 8 more than the second place, achieving top-1 performance. Second, our method is suitable for data containing arbitrary-shaped clusters. For instance, the clusters in datasets "S2"(Fig. 2(a)), "A1"(Fig. 2(b)),

⁴ <http://cs.joensuu.fi/sipu/datasets/>

⁵ <http://www.cs.toronto.edu/~kriz/cifar.html>

⁶ <https://cs.stanford.edu/~acoates/stl10/>

⁷ <http://yann.lecun.com/exdb/mnist/>

⁸ <http://www.prima.inrialpes.fr/Pointing04>

Table 1: Basic information about the studied data sets.

Name	Size	Dimension	Class	Description
Unbalanced	1500	2	3	Multi-density
Flame	240	2	2	Overlapping
Jain	373	2	2	Crescent, Multi-density
S2	5000	2	15	Sub-cluster, Overlapping
A1	3000	2	20	Small cluster
Asymmetric	1000	2	5	Unbalanced, noisy
Heterogeneous	400	2	3	Heterogeneous geometric
Multi-objective	1000	2	4	elongated, circle-like, multi-objective
REUTERS-10K	10000	12000	4	Word, News, Text,
Covid-19	171	53	3	Covid-19
RNA-seq	801	20531	5	Gene expression, Nonlinear
MNIST	10000	28*28	10	OCR, high-dimensional
Pendigits	10992	4*4	10	Handwritten Digits
Optical Recognition	5620	64	10	OCR, Handwritten Digits
Pointing Data	1395	384*284*3	15	Posture recognition
STL-10	13000	3*96*96	10	Complex Contextual
CIFAR-10	10000	3*32*32	10	Complex Contextual, Large-Scale

"Flame"(Fig. 2(d)), and "Asymmetric"(Fig. 2(f)) almost overlap visually. Whereas datasets "Unbalanced"(Fig. 2(c)) and "Jain"(Fig. 2(e)) are examples of multi-density, showing manifold and unbalanced, respectively. As a result, only our method accurately identified all of them. Besides, Table 2 also reports the more challenging datasets from real world. For example, REUTERS-10K is a typical text type; Covid-19 records biochemical indicators of 3 types of COVID-19 with significant dimensional-difference; RNA-seq records a surprising 20,000 dimensions of gene transcription data. The six large-scale image datasets further validate the effectiveness of our algorithm CNMBI, especially for complex CIFAR-10 and STL-10, where only CNMBI achieves the correct cluster number estimation. The above satisfactory performance is mainly thanks to the joint modeling of the center pairwise matching scheme and the boundary filtering principle, the former ensuring the flexibility of our method in terms of data dimension and shape, while the latter enhancing the robustness of CNMBI when handling complex data. It is also worth mentioning that the scores under the ACC metric indicate that our method is more stable than other methods over multiple runs. In particular, Fig. 3 visualizes the optimization process of part of the data set.

4.2 Ablation Study

Table 3 reports the experimental results, from which we can draw some conclusions: 1) Method-1 removes the boundary filtering strategy compared to our method, resulting in a significant decrease in NC score from a perfect score of 1 to 0.2 on the Pointing Dataset, which demonstrates that this strategy plays an important role in improving robustness; 2) The results of Method-5 indicate

that our method has good scalability, i.e., cluster number identification can also be achieved by comparing the mean centers generated twice, although it is not as stable as our original method, as in the case of NC score.

Table 2: Cluster number prediction on challenging datasets over 50 runs.

Dataset	SC		DPC-AHS		VCIM		LCCV		CNAK		CNMBI	
	NC	ACC	NC	ACC	NC	ACC	NC	ACC	NC	ACC	NC	ACC
Unbalanced	2	0	2	0	2	0	2	0	3	0.9	3	1
Flame	4	0	2	1	4	0	4	0	1	0	2	1
Jain	2	0.5	2	1	3	0	7	0	3	0	2	1
S2	15	0.4	13	0	2	0	23	0	15	1	15	1
A1	20	0.1	20	1	2	0	4	0	20	1	20	1
Asymmetric	2	0	5	1	2	0	5	1	5	0.5	5	1
Heterogeneous	2	0	2	0	5	0	4	0	2	0	3	1
Multi-objective	12	0	2	0	3	0	4	1	3	0	4	1
REUTERS-10K	78	0	4	1	2	0	92	0	1	0	4	0.1
Covid-19	2	0	3	1	3	1	2	0	3	1	3	1
RNA-seq	5	0.6	5	1	5	1	5	1	5	0.6	5	1
MNIST	10	0.1	8	0	3	0	10	1	10	0.1	10	1
Pendigits	15	0	13	0	2	0	13	0	11	0	10	0.8
Optical	10	0.7	5	0	7	0	10	1	10	1	10	1
Pointing Data	14	0	25	0	3	0	24	0	9	0	15	1
STL-10	20	0	1	0	-	-	-	-	1	0	10	0.2
CIFAR-10	1	0	1	0	-	-	56	0	10	0.1	10	0.3

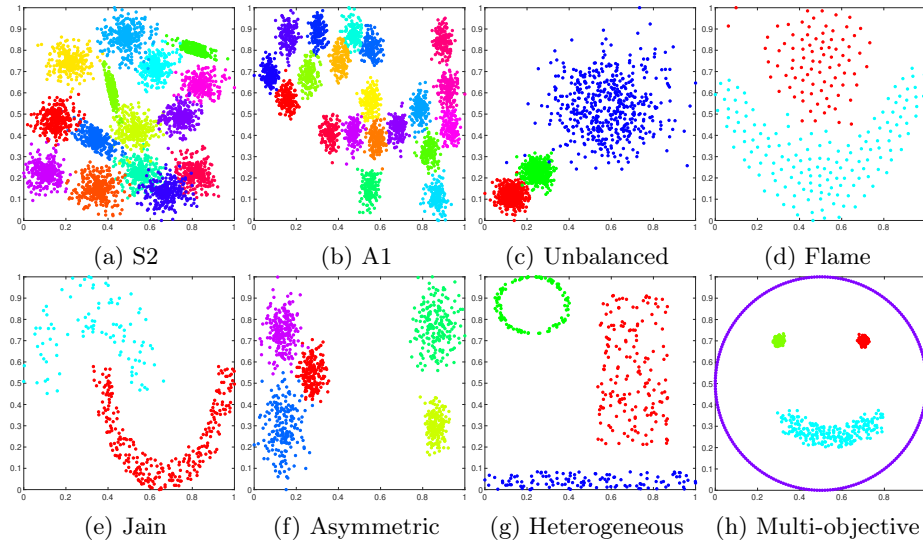
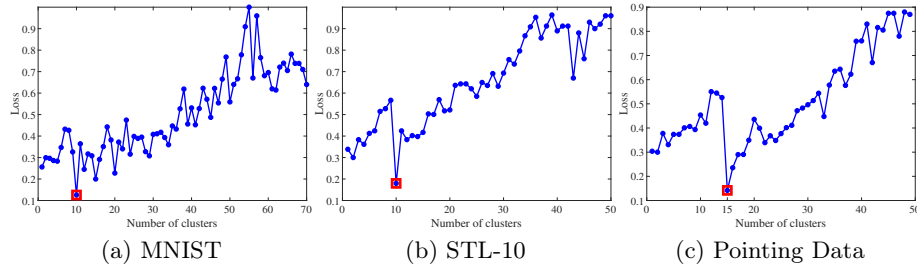


Fig. 2: Synthetic dataset containing arbitrary-shaped clusters.

Fig. 3: Plots of k and center pairwise loss on partial image data sets.Table 3: Ablation study of CNMBI and its degradation methods. S_μ , S_γ and φ denote the Mean center, Denisty center, and boundary filtering, respectively.

Methods	S_μ	S_γ	φ	MNIST		Pointing Data	
Ours	✓	✓	✓	NC: 10	ACC: 1	NC: 15	ACC: 1
Method-1	✓	✓	×	NC: 10	ACC: 0.6	NC: 15	ACC: 0.2
Method-2	✓	×	×	NC: 1	ACC: 0	NC: 1	ACC: 0
Method-3	×	✓	×	NC: 10	ACC: 0.3	NC: 15	ACC: 0.1
Method-4	✓	×	✓	NC: 1	ACC: 0	NC: 1	ACC: 0
Method-5	×	✓	✓	NC: 10	ACC: 0.5	NC: 15	ACC: 0.4

4.3 Parameter Sensitivity

CNMBI is parameter-free since the parameters, cutoff distance dc in density center and proportion λ in boundary filtering, are dynamically adaptive. Here we test CNMBI in three typical scenarios, each with four datasets, as reported in Fig. 4. For scenario "Noise," different levels of noise interference are added. The "Density" consists of 8 clusters with unbalanced density. For "Number," the four data sets contained have different numbers of clusters, 5,10,20,40.

The results are concentrated in Fig. 4(m). Concretely, as given by the red line in Fig. 4, it can be found that from the first to the fourth dataset, CNMBI behaves satisfactorily without error despite the increase in the number of clusters. The Noise-40 and Noise-50 dataset (Fig. 4(g),(h)) cannot be visually separated due to intense noise disturbance, CNMBI can still determine the desired number of clusters 2 (see the blue-green line segment in Fig. 4). Moreover, the density imbalance gradually increases from Density-1 to Density-4, and the green line segment in Fig. 4 shows that CNMBI is robust to density changes. Generally, benefiting from the consideration of active boundary filtering and simple but effective cluster number features generated by center matching, CNMBI has better robustness against data with complex distribution than other methods.

4.4 Boundary Pattern Recognition

Our method can extract valuable boundary pattern information while determining the number of clusters. Although some points cause undesirable results in cluster number determination, in practice, these objects often possess the characteristics of two or more groups simultaneously and have great potential value, such as populations carrying viruses but not manifested in epidemiology and scribbled characters in optical character recognition.

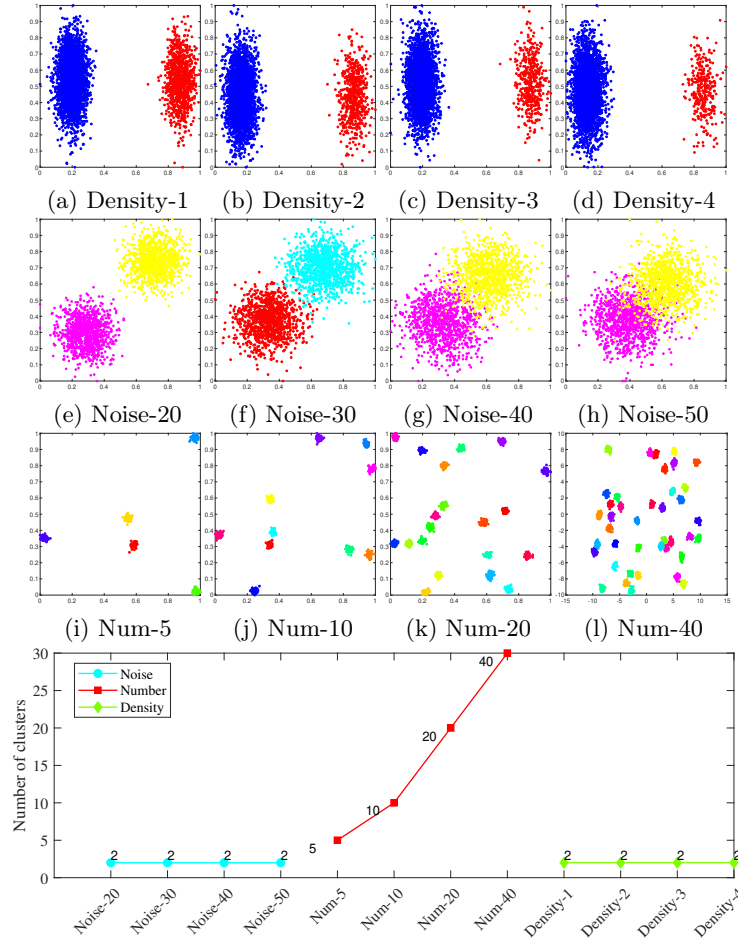


Fig. 4: Three extreme scenarios in Robustness

Fig. 5(a) shows the boundary samples we extracted from the handwriting dataset (MNIST), from which it can be seen that the characters are illegible, with blurred, hollow, continuous strokes that are distinctly different from normal fonts. The pointing dataset records 23 types of head posture images from 15 volunteers. As shown in Fig. 5(b), the identified images have exaggerated move-

ments and complex expressions from Pointing Data, which is beneficial for determining the amplitude threshold of each action in the pose recognition. Moreover, our proposed boundary filtering method is informative for other learning tasks.

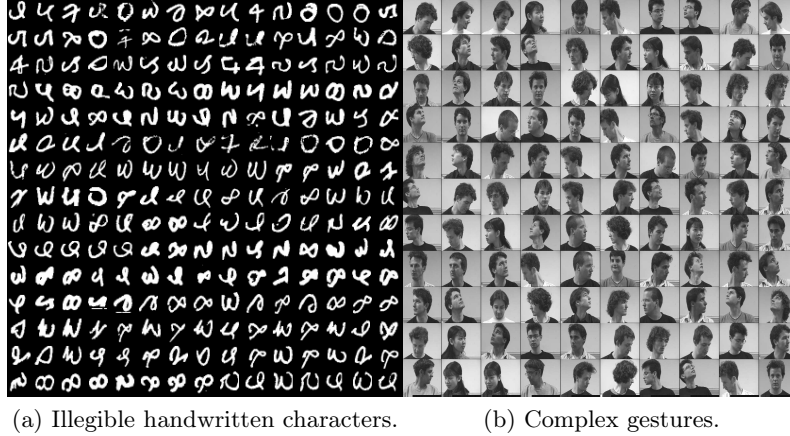


Fig. 5: Boundary pattern information extraction.

5 Discussion

In this section, we provide a deeper introspection into the structural mechanics of CNMBI and explore its conceptual evolution towards broader learning paradigms.

5.1 Introspection of CNMBI Mechanics

Breaking Isotropic Assumptions via Dual-Center Coupling. The fundamental limitation of conventional cluster validity indices is their implicit reliance on the assumption of isotropic, convex data distributions. Most methods evaluate the "goodness" of a partition by measuring inter-cluster separation and intra-cluster compactness. However, real-world data manifolds are often non-convex and characterized by varying densities, rendering distance-based compactness uninformative.

CNMBI moves beyond this by introducing a *Dual-Center Coupling* mechanism. Instead of scoring the final partition, we examine the structural alignment between the *density center* (representing the topological core) and the *mean center* (representing the geometric centroid).

We observe that in a suboptimal clustering state ($k \neq K$), the geometric centroid is easily skewed by partial cluster merging or splitting, while the topological core remains relatively stable. The "Center Pairwise Loss" essentially quantifies this structural tension. By seeking the global minimum of this loss, CNMBI effectively identifies the number of clusters where the geometric and topological

perspectives reach a state of equilibrium, allowing for a robust determination of K without a priori assumptions about the cluster shape.

Boundary Filtering as Pattern Purification. A critical bottleneck in unsupervised number determination is "centroid drift" caused by low-confidence samples located at the fringes of clusters or within overlapping regions. In high-dimensional spaces, these boundary points act as "noise" that blurs the distinctiveness of clusters.

CNMBI addresses this via a boundary filtering module grounded in *Space Vector Decomposition*. Unlike standard outlier detection, which often focuses on global distance, our approach evaluates the *positional belief* of a sample based on the asymmetry of its local neighborhood vector. By projecting these vectors onto an orthogonal basis, we can identify samples that exist in high-entropy transition zones. Filtering these samples is not merely a denoising step but a process of **Pattern Purification**. By isolating the "cluster skeleton," we ensure that the subsequent center matching is conducted on the most stable and representative core of the data, significantly enhancing the precision of the loss function.

Metric Generalization and Manifold Scalability. From a structural standpoint, the pairwise matching framework in CNMBI is not strictly bound to Euclidean geometry. The algorithm's architecture suggests a generalized framework where the similarity between the dual centers can be redefined through diverse metric spaces:

- **Manifold Consistency:** The matching process can be viewed as an attempt to find the point where the local manifold density peak aligns with the global cluster mass. This suggests that the framework is naturally scalable to non-linear manifolds where traditional L_2 norms may fail.
- **Metric Flexibility:** The "Center Pairwise Loss" serves as a meta-objective that can incorporate different distance or similarity measures depending on the data modality. By focusing on the *behavioral behavior* of centers rather than the *assignment of every single point*, CNMBI provides a computationally efficient and theoretically flexible pathway for identifying structures in ultra-high-dimensional or distorted feature spaces.

5.2 Evolution Toward Open-World Discovery and Cross-Domain Applications

Paving the Way for Open-World Perception. The robust estimation of cluster counts is a transformative cornerstone for transitioning from static clustering to the dynamic Open-World paradigm. A major bottleneck in Generalized Category Discovery [61] and On-the-fly Category Discovery [60] is the unrealistic assumption that the number of novel or fine-grained categories is known a priori. By synergizing CNMBI with Transformer-based global dependency modeling [55], curriculum-driven density core assignments [62], and multi-modality co-teaching [61], future architectures can achieve a more holistic and autonomous understanding of evolving data streams without human-in-the-loop parameter

tuning. Beyond discovery, this autonomous capability extends naturally to data-efficient learning and generative modeling. By dynamically capturing the underlying number of semantic modes in complex distributions, the proposed logic can provide critical structural guidance for adaptive dataset quantization [14] and diverse dataset distillation frameworks [17,16,15], ensuring that synthetic or compressed proxies preserve the full topological and categorical diversity of the original data. Similarly, recognizing the true scale of latent cluster densities can enhance data-free knowledge distillation by anchoring diverse diffusion-based augmentations [18] to precise semantic centers. Finally, moving towards advanced 3D generative vision, these density-aware structural priors hold significant potential to refine probability density flow matching, enabling more stable and mode-preserving geodesic estimations for novel view synthesis [46].

Cross-Domain Potential and Future Trajectories. CNMBI effectively addresses the pre-definition limitation of classical clustering algorithms by automating the estimation of cluster counts, thereby serving as a robust initialization engine for diverse downstream pipelines. For medical imaging, it facilitates pathological region partitioning by automatically determining the number of distinct tissue layers or lesion types in OCT images, which is essential for guided denoising and segmentation [21,20,19,22]. In 3D vision, CNMBI enhances global solvers and vanishing point estimation [59,57,58,26] by discovering the true number of geometric directions in unstructured environments, and streamlines instance-level point cloud grouping [31,32,30]. For robotics, it automates the identification of latent physical modes (e.g., estimating the number of slip, rotation, or stable contact states) within tactile or sensor data streams, thereby refining stability analysis and cooperative control [51,36,50,52,48,44]. In embodied AI and video-language modeling, CNMBI aids in temporal event partitioning by clustering video segments into an adaptive number of semantic events [23], and assists in defining the optimal granularity for action primitives in VLA models [24], establishing the structured semantic groundwork necessary for deliberate System-2 reasoning capabilities [41]. Furthermore, it optimizes knowledge distillation by providing the precise cluster scale for location-aware semantic masking [8,9,7], and yields aligned structural counts that can effectively bridge semi-supervised domain translation via diffusion models [47]. Finally, CNMBI provides a scalable way to estimate entity counts in open-vocabulary marine or remote sensing segmentation [10,13,12,11] and identifies structural group counts in socio-meteorological analysis [27,39,40]. In this paper, we propose a novel method, CNMBI, to identify the number of clusters, which is capable of being applied to some challenging data such as large-scale images and high-dimensional real-world data. We are the first to report the results on STL-10 and CIFAR-10. We do not rely on the clustering results of the entire data but instead utilize a few but highly representative cluster centers. This purposely straightforward contrast allows our method to be more scalable and flexible in dimension and shape, most importantly, sufficient for discovering actual cluster numbers through the positional behavior of the cluster center. Additionally, the

principle of filtering low-confidence samples further enhances the robustness of our method, which is the first attempt in this field.

Acknowledgements This work was supported in part by the Shenzhen Fundamental Research Fund (JCYJ20210324132212030) and the Guangdong Provincial Key Laboratory of Novel Security Intelligence Technologies (2022B1212010005).

References

1. Abdalameer, A.K., Alswaitti, M., Alsudani, A.A., Isa, N.A.M.: A new validity clustering index-based on finding new centroid positions using the mean of clustered data to determine the optimum number of clusters. *Expert Systems with Applications* **191**, 116329 (2022)
2. Bache, K., Lichman, M.: Uci machine learning repository (2013), <https://doi.org/10.1145/2063576.2063689>
3. Calinski, T., Harabasz, J.: A dendrite method for cluster analysis. *Communications in Statistics* **3**, 1–27 (01 1974). <https://doi.org/10.1080/03610917408548446>
4. Cheng, D., Zhu, Q., Huang, J., Wu, Q., Yang, L.: A novel cluster validity index based on local cores. *IEEE Transactions on Neural Networks and Learning Systems* **30**(4), 985–999 (2019). <https://doi.org/10.1109/TNNLS.2018.2853710>
5. Davies, D.L., Bouldin, D.W.: A cluster separation measure. *IEEE Transactions on Pattern Analysis and Machine Intelligence* **PAMI-1**(2), 224–227 (1979)
6. Dunn, J.C.: A fuzzy relative of the isodata process and its use in detecting compact well-separated clusters. *Journal of Cybernetics* **3**(3), 32–57 (1973)
7. Lan, Q., Tian, Q.: Gradient-guided knowledge distillation for object detectors. In: *Proceedings of the IEEE/CVF Winter Conference on Applications of Computer Vision*. pp. 424–433 (2024)
8. Lan, Q., Tian, Q.: Acam-kd: adaptive and cooperative attention masking for knowledge distillation. In: *Proceedings of the IEEE/CVF International Conference on Computer Vision*. pp. 3957–3966 (2025)
9. Lan, Q., Tian, Q.: Clockdistill: Consistent location and context aware knowledge distillation for detr. In: *Proceedings of the IEEE/CVF Winter Conference on Applications of Computer Vision*. pp. 7188–7197 (2026)
10. Li, B., Dong, H., Zhang, D., Zhao, Z., Gao, J., Li, X.: Exploring efficient open-vocabulary segmentation in the remote sensing. *arXiv preprint arXiv:2509.12040* (2025)
11. Li, B., Huo, T., Zhang, D., Zhao, Z., Gao, J., Li, X.: Exploring the underwater world segmentation without extra training. *arXiv preprint arXiv:2511.07923* (2025)
12. Li, B., Wang, F., Zhang, D., Zhao, Z., Gao, J., Li, X.: Maris: Marine open-vocabulary instance segmentation with geometric enhancement and semantic alignment. *arXiv preprint arXiv:2510.15398* (2025)
13. Li, B., Zhang, D., Zhao, Z., Gao, J., Li, X.: Stitchfusion: Weaving any visual modalities to enhance multimodal semantic segmentation. In: *Proceedings of the 33rd ACM International Conference on Multimedia*. pp. 1308–1317 (2025)
14. Li, M., Zhang, D., Dong, Q., et al.: Adaptive dataset quantization. In: *Proceedings of the AAAI Conference on Artificial Intelligence*. vol. 39, pp. 12093–12101 (2025)
15. Li, M., Dong, Q., Zhang, D., Qin, K., Luo, G.: Efficient industrial dataset distillation with textual trajectory matching. *IEEE Transactions on Industrial Informatics* (2026)

16. Li, M., Gou, H., Ma, Y., Wang, R., Qin, K., He, T.: Fixed anchors are not enough: Dynamic retrieval and persistent homology for dataset distillation. arXiv preprint arXiv:2602.24144 (2026)
17. Li, M., Gou, H., Zhang, D., Liang, S., Xie, X., Ouyang, D., Qin, K.: Beyond random: Automatic inner-loop optimization in dataset distillation. In: NeurIPS (2025)
18. Li, M., Zhang, D., He, T., Xie, X., Li, Y., Qin, K.: Towards effective data-free knowledge distillation via diverse diffusion augmentation. In: Proceedings of the 32nd ACM International Conference on Multimedia, MM. pp. 4416–4425 (2024)
19. Li, S., Chu, Y., Zhao, Y., Zhao, P.: An efficient deep learning-based framework for image distortion correction. *The Visual Computer* **40**(10), 6955–6967 (2024)
20. Li, S., Dan, M., Chu, Y., Yu, J., Zhao, Y., Zhao, P.: Retidiff: Diffusion-based synthesis of retinal oct images for enhanced segmentation. In: International Conference on Medical Image Computing and Computer-Assisted Intervention. pp. 516–525. Springer (2025)
21. Li, S., Dan, M., Chu, Y., Zhao, Y., Zhao, P.: Cross-domain knowledge integration framework for optical coherence tomography images denoising. *Biomedical Signal Processing and Control* **113**, 108916 (2026)
22. Li, S., Zhao, Y., Zhao, P.: Garnet: Geometry-aware rectification network for generic image distortions. *Knowledge-Based Systems* p. 115632 (2026)
23. Li, W., Hu, B., Shao, R., Shen, L., Nie, L.: Lion-fs: Fast & slow video-language thinker as online video assistant. In: Proceedings of the IEEE/CVF Conference on Computer Vision and Pattern Recognition. pp. 3240–3251 (2025)
24. Li, W., Zhang, R., Shao, R., He, J., Nie, L.: Cogvla: Cognition-aligned vision-language-action model via instruction-driven routing & sparsification. In: Advances in Neural Information Processing Systems (2025)
25. Li, Y., Hu, P., Liu, Z., Peng, D., Zhou, J.T., Peng, X.: Contrastive clustering. Proceedings of the AAAI Conference on Artificial Intelligence **35**(10), 8547–8555 (May 2021). <https://doi.org/10.1609/aaai.v35i10.17037>
26. Liao, B., Zhao, Z., Li, H., Zhou, Y., Zeng, Y., Li, H., Liu, P.: Convex relaxation for robust vanishing point estimation in manhattan world. In: Proceedings of the Computer Vision and Pattern Recognition Conference. pp. 15823–15832 (2025)
27. Liu, D., Shen, Q., Liu, J.: The health-wealth gradient in labor markets: Integrating health, insurance, and social metrics to predict employment density. *Computation* **14**(1), 22 (2026)
28. Nguyen, S.D., Nguyen, V.S.T., Pham, N.T.: Determination of the optimal number of clusters: A fuzzy-set based method. *IEEE Transactions on Fuzzy Systems* **30**(9), 3514–3526 (2022). <https://doi.org/10.1109/TFUZZ.2021.3118113>
29. Qiu, T., Li, Y.: Fast ldp-mst: an efficient density-peak-based clustering method for large-size datasets. *IEEE Transactions on Knowledge and Data Engineering* pp. 1–1 (2022)
30. Qu, W., Mei, G., Wang, J., Wu, Y., Huang, X., Xiao, L.: Robust single-stage fully sparse 3d object detection via detachable latent diffusion. arXiv preprint arXiv:2508.03252 (2025)
31. Qu, W., Shao, Y., Meng, L., Huang, X., Xiao, L.: A conditional denoising diffusion probabilistic model for point cloud upsampling. In: Proceedings of the IEEE/CVF Conference on Computer Vision and Pattern Recognition. pp. 20786–20795 (2024)
32. Qu, W., Wang, J., Gong, Y., Huang, X., Xiao, L.: An end-to-end robust point cloud semantic segmentation network with single-step conditional diffusion models. In: Proceedings of the Computer Vision and Pattern Recognition Conference. pp. 27325–27335 (2025)

33. Rasool, Z., Zhou, R., Chen, L., Liu, C., Xu, J.: Index-based solutions for efficient density peak clustering. *IEEE Transactions on Knowledge and Data Engineering* **34**(5), 2212–2226 (2022). <https://doi.org/10.1109/TKDE.2020.3004221>
34. Rodriguez, A., Laio, A.: Clustering by fast search and find of density peaks. *Science* **344**(6191), 1492–1496 (2014). <https://doi.org/10.1126/science.1242072>
35. Rousseeuw, P.J.: Silhouettes: A graphical aid to the interpretation and validation of cluster analysis. *Journal of Computational and Applied Mathematics* **20**, 53–65 (1987). [https://doi.org/https://doi.org/10.1016/0377-0427\(87\)90125-7](https://doi.org/https://doi.org/10.1016/0377-0427(87)90125-7)
36. Ruan, Z., Yan, T., Cai, Y., Han, Y., Zheng, L., Zhang, Y.: Q-value regularized decision convformer for offline reinforcement learning. In: 2024 IEEE International Conference on Robotics and Biomimetics (ROBIO). pp. 91–97. IEEE (2024)
37. Saha, J., Mukherjee, J.: Cnak: Cluster number assisted k-means. *Pattern Recognition* **110**, 107625 (2021)
38. Salvador, S., Chan, P.: Determining the number of clusters/segments in hierarchical clustering/segmentation algorithms. In: 16th IEEE International Conference on Tools with Artificial Intelligence. pp. 576–584 (2004)
39. Shen, Q., Zhang, J.: Ai-enhanced disaster risk prediction with explainable shap analysis: A multi-class classification approach using xgboost (December 2025). <https://doi.org/10.21203/rs.3.rs-8437180/v1>, <https://www.researchsquare.com/article/rs-8437180/v1>, preprint, Version 1, posted December 31, 2025
40. Shen, Q., Zhang, J.: Mftformer: Meteorological-frequency-temporal transformer with block-aligned fusion for traffic flow prediction. *Research Square* (2026), preprint, doi:10.21203/rs.3.rs-8770196/v1
41. Song, H., Qu, D., Yao, Y., Chen, Q., Lv, Q., Tang, Y., Shi, M., Ren, G., Yao, M., Zhao, B., et al.: Hume: Introducing system-2 thinking in visual-language-action model. *arXiv preprint arXiv:2505.21432* (2025)
42. Sugar, C.A., James, G.M.: Finding the Number of Clusters in a Dataset: An Information-Theoretic Approach. *Journal of the American Statistical Association* **98**, 750–763 (January 2003)
43. Tavakkol, B., Choi, J., Jeong, M.K., Albin, S.L.: Object-based cluster validation with densities. *Pattern Recognition* **121**, 108223 (2022)
44. Tian, A.X., Zhang, R., Tang, J., Wang, J., Shi, T., Wen, J.: Measuring harmfulness of computer-using agents. *arXiv preprint arXiv:2508.00935* (2025)
45. Tibshirani, R., Walther, G., Hastie, T.: Estimating the number of clusters in a data set via the gap statistic. *Journal of the Royal Statistical Society Series B* **63**(2), 411–423 (2001). <https://doi.org/10.1111/1467-9868.00293>
46. Wang, X., Wu, T., Zhang, Y., Liu, L., Sun, M., Wang, Y., Zeller, N., Cremers, D.: Geodesicnvs: Probability density geodesic flow matching for novel view synthesis. *arXiv preprint arXiv:2603.01010* (2026)
47. Wang, X., Wu, T., Zhang, Y., Liu, L., Wang, D., Sun, M., Wang, Y., Zeller, N., Cremers, D.: Ladb: Latent aligned diffusion bridges for semi-supervised domain translation. In: DAGM German Conference on Pattern Recognition. pp. 221–236. Springer (2025)
48. Xu, H., Hu, J., Zhang, K., Yu, L., Tang, Y., Song, X., Duan, Y., Ai, L., Shi, B.: Sedm: Scalable self-evolving distributed memory for agents. *arXiv preprint arXiv:2509.09498* (2025)
49. Xu, X., Ding, S., Wang, L., Wang, Y.: A robust density peaks clustering algorithm with density-sensitive similarity. *Knowledge-Based Systems* **200**, 106028 (2020)

50. Yan, T., Sun, Y., Zhang, Y., Yu, Z., Li, W., Zhang, K.: Stability analysis of 3c electronic industry robot grasping based on visual-tactile sensing. In: 2023 3rd International Conference on Robotics, Automation and Artificial Intelligence (RAAI). pp. 183–188. IEEE (2023)
51. Yan, T., Zhou, X., Long, J., Li, W., Zhang, Y.: Pandas: Prediction and detection of accurate slippage. In: 2025 IEEE/RSJ International Conference on Intelligent Robots and Systems (IROS). pp. 2827–2834. IEEE (2025)
52. Zhang, M., Fang, Z., Wang, T., Lu, S., Wang, X., Shi, T.: Ccma: A framework for cascading cooperative multi-agent in autonomous driving merging using large language models. *Expert Systems with Applications* **282**, 127717 (2025)
53. Zhang, R., Miao, Z., Tian, Y., Wang, H.: A novel density peaks clustering algorithm based on hopkins statistic. *Expert Systems with Applications* **201**, 116892 (2022)
54. Zhang, R., Zheng, H.: Density clustering based on the border-peeling using space vector decomposition. *Acta Automatica Sinica* **49**(6), 1–19 (2023)
55. Zhang, R., Zheng, H., Wang, H.: Tdec: Deep embedded image clustering with transformer and distribution information. In: Proceedings of the 2023 ACM International Conference on Multimedia Retrieval. pp. 280–288 (2023)
56. Zhang, Y., Mańdziuk, J., Quek, C.H., Goh, B.W.: Curvature-based method for determining the number of clusters. *Information Sciences* **415–416**, 414–428 (2017)
57. Zhao, Z.: Balf: Simple and efficient blur aware local feature detector. In: Proceedings of the IEEE/CVF Winter Conference on Applications of Computer Vision. pp. 3362–3372 (2024)
58. Zhao, Z., Chen, B.M.: Benchmark for evaluating initialization of visual-inertial odometry. In: 2023 42nd Chinese Control Conference (CCC). pp. 3935–3940. IEEE (2023)
59. Zhao, Z., Yang, H., Liao, B., Zeng, Y., Yan, S., Gu, Y., Liu, P., Zhou, Y., Li, H., Civera, J.: Advances in global solvers for 3d vision. arXiv preprint arXiv:2602.14662 (2026)
60. Zheng, H., Pu, N., Li, W., Sebe, N., Zhong, Z.: Prototypical hash encoding for on-the-fly fine-grained category discovery. *Advances in Neural Information Processing Systems* **37**, 101428–101455 (2024)
61. Zheng, H., Pu, N., Li, W., Sebe, N., Zhong, Z.: Textual knowledge matters: Cross-modality co-teaching for generalized visual class discovery. In: European Conference on Computer Vision. pp. 41–58. Springer (2024)
62. Zheng, H., Zhang, R., Wang, H.: Deep image clustering based on curriculum learning and density information. In: Proceedings of the 2024 International Conference on Multimedia Retrieval. pp. 330–338 (2024)